Chatterjee, Dheeman and Ghosh, Arindam (2007) Transient Stability Assessment of Power Systems Containing Series and Shunt Compensators. *IEEE Transactions on Power Engineering* 22(3):pp. 1210-1220.

Transient Stability Assessment of Power Systems Containing Series and Shunt Compensators

Dheeman Chatterjee, *Student Member, IEEE*, and Arindam Ghosh, *Fellow, IEEE*

***Abstract*—This paper discusses the application of trajectory sensitivity analysis (TSA) of power systems containing FACTS compensators. Thyristor controlled series compensator (TCSC) and static synchronous compensator (STATCOM) are the devices considered. The TCSC is modeled by a variable capacitor, the value of which changes with the firing angle. The STATCOM is modeled by a voltage source connected to the system through a transformer. The effect of their individual and simultaneous use on the system transient stability is studied by applying TSA. Two different test systems are considered. It is shown that TSA can be used to determine the best possible locations of the two devices for transient stability improvement as well as to predict the critical clearing time.**

***Index Terms*—Optimal location, static synchronous compensator (STATCOM), thyristor controlled series compensator (TCSC), trajectory sensitivity analysis, transient stability margin.**

I. Introduction

THE ELECTRICAL energy industry is presently undergoing restructuring and deregulation in different parts of the world. This is expected to bring in more competition between utilities. So the improvement of power system operation efficiency is a requirement from the operational point of view. The available system will be pushed to its limits, and hence, maintaining system reliability will be of increasing importance. FACTS devices help in increasing the operational efficiency of power systems without affecting the reliability of supply. Series compensation devices like thyristor controlled series compensator (TCSC) and shunt compensation devices like static synchronous compensator (STATCOM) help in increasing the transient stability margin of power systems and thus provide means to operate the system near their limits. However, for large power systems, more than one compensator may be required to achieve the targeted performance. Therefore, detailed prior knowledge about the effect of simultaneous application of more than one FACTS device in different locations of a system is required.

Assessment of transient stability condition of the system is essential for understanding the effect of application of FACTS devices. The transient energy function (TEF) method is the standard tool used for this purpose. Analytical sensitivity of transient energy margin has been used to compute the stability limits of power systems in [1]. The effectiveness of individual FACTS compensators on transient stability has been studied using structure preserving energy margin sensitivity also in [2]. However, the TEF-based methods may become too complex when a detailed model, including FACTS device, is considered, and a number of parameters have to be taken into account. The computation of controlling unstable equilibrium point (UEP) may pose increased computational problems.

Trajectory sensitivity (TS) has been proposed as an alternative to the TEF-based methods in [3]. Trajectory sensitivities can be computed numerically, which is a big advantage if dynamic models of devices are considered. Trajectory sensitivity in finding critical values of parameters, dynamic rescheduling of generation, as well as other applications have been reported in the literature [4]–[6]. A method to reduce the number of TS calculations is discussed in [7].

Mathematical modeling and analysis of static compensator (STATCOM) is presented in [8]. It discusses the use of STATCOM in improvement of transient stability and power transfer. The TCSC can also be placed in one of the lines of a power system with suitable control scheme to improve the transient stability condition of the system [9].

In this paper, TSA has been used to study the effects of FACTS controllers on the transient stability of a power system. Sensitivity with respect to fault clearing time has been considered. At first, a series compensator (TCSC) and a shunt compensator (STATCOM) are placed individually, and the post-fault stability condition is studied. The effects of variation in the locations of fault and FACTS devices as well as changes in the values of FACTS device parameters are studied. The TCSC is represented by a fundamental frequency lumped reactance model, the value of the reactance varying with the change in the firing angle. The STATCOM is represented by a voltage source, which is connected to the system through a coupling transformer. The voltage of the source is in phase with the ac system voltage at the point of connection, and the magnitude of the voltage is controllable. The current from the source is limited to a maximum value by adjusting the voltage. In the next step, two FACTS devices are placed simultaneously at two different locations of the system. The effects of individual shunt and series compensation and simultaneous compensation are compared. Effects of compensation in a stressed system are also studied. The systems under consideration are the three-machine, nine-bus WSCC system [10] and the IEEE 16-machine 68-bus system [11]. System load is considered as constant PQ. The method can be easily extended to handle other load models, like constant impedance, etc.

Manuscript received January 10, 2006; revised December 6, 2006. Paper no. TPWRS-00012-2006.

D. Chatterjee is with the Department of Electrical Engineering, Indian Institute of Technology Kanpur, Uttar Pradesh 208016, India.

A. Ghosh is with the School of Engineering Systems, Queensland University of Technology, Brisbane, Queensland 4001, Australia.

Color versions of one or more of the figures in this paper are available online at http://ieeexplore.ieee.org.

Digital Object Identifier 10.1109/TPWRS.2007.901455

II. Trajectory Sensitivity Analysis of Multimachine Power System

A. Trajectory Sensitivity Analysis

Suppose a multimachine power system is represented by the set of differential and algebraic equations given as

$$\begin{aligned} \dot{x} &= f(x, y, \lambda), \quad x(t_0) = x_0 \\ 0 &= g(x, y, \lambda), \quad y(t_0) = y_0 \end{aligned} \tag{1}$$

where x is the state vector, y is a vector of algebraic variables, and λ is a vector of system parameters. Then the sensitivities of state trajectories with respect to system parameters can be found by perturbing λ from the nominal value of λ_0. The equations for TS can be found as [3]

$$\begin{aligned} \dot{w}_1 &= \left[\frac{\partial f}{\partial x}\right] w_1 + \left[\frac{\partial f}{\partial y}\right] w_2 + \left[\frac{\partial f}{\partial \lambda}\right], \quad w_1(t_0) = 0 \\ 0 &= \left[\frac{\partial g}{\partial x}\right] w_1 + \left[\frac{\partial g}{\partial y}\right] w_2 + \left[\frac{\partial g}{\partial \lambda}\right], \quad w_2(t_0) = 0 \end{aligned} \tag{2}$$

where $w_1 = \partial x/\partial\lambda$ and $w_2 = \partial y/\partial\lambda$ are the sensitivities. Solving (1) and (2) simultaneously, we get x, y and the sensitivities w_1 and w_2.

However, the TS can also be found in a simpler way by using a numerical method. Let us choose one scalar parameter λ and compute the sensitivities with respect to it. Two values of λ are chosen (say, λ_1 and λ_2), and the corresponding state vectors x_1 and x_2, respectively, are computed. Now the sensitivity at λ_1 is defined as

$$\text{Sens} = \frac{x_2 - x_1}{\lambda_2 - \lambda_1} = \frac{\Delta x}{\Delta \lambda}. \tag{3}$$

By taking $\Delta\lambda$ small, the numerical sensitivity is very close to the analytically calculated trajectory sensitivity value.

B. Multimachine Power System Model

Consider an n-bus, m-machine system with the machines represented by classical model (i.e., a voltage of constant magnitude behind the transient reactance of the machine). The buses are numbered 1 to n, and the internal nodes of the machines are represented by $(n+1)$ to $(n+m)$. The swing equations are given as [12] for $i = n+1, \ldots, n+m$

$$\frac{d\theta_i}{dt} = \omega_s \Delta\omega_{r_i} \tag{4}$$

$$\begin{aligned} 2H_i \frac{d\Delta\omega_{r_i}}{dt} = P_{m_i} - \sum_{j=1}^{n+m} |V_i| \cdot |V_j| [G_{ij} \cos(\theta_i - \theta_j) \\ + B_{ij} \sin(\theta_i - \theta_j)] - K_{D_i} \Delta\omega_{r_i} \end{aligned} \tag{5}$$

where $\Delta\omega_r$ is the per unit speed deviation, H is the inertia constant, ω_s is the synchronous speed, m is the number of machines, P_m the mechanical power input in per unit, $V_i (i = 1 \cdots n)$ are the bus voltages in per unit, and $\theta_i (i = 1 \ldots n)$ are the phase angles in radians. Here $\theta_i (i = n+1 \ldots n+m)$ are the δ_i's, the angular positions of the rotors and $V_i (i = n+1 \cdots n+m)$ are the constant magnitudes of internal voltages of the machines. The dynamics of the network and the stator windings are neglected, and the network is represented by a set of algebraic equations for $i = 1, \ldots, n$

$$P_{L_i} = \sum_{j=1}^{n+m} |V_i||V_j|[G_{ij} \cos(\theta_i - \theta_j) + B_{ij} \sin(\theta_i - \theta_j)] \tag{6}$$

$$Q_{L_i} = \sum_{j=1}^{n+m} |V_i||V_j|[G_{ij} \sin(\theta_i - \theta_j) - B_{ij} \cos(\theta_i - \theta_j)] \tag{7}$$

where G_{ij} and B_{ij} are the network transfer conductance and admittance, respectively. These are obtained from the augmented Y_{BUS} matrix where the admittance corresponding to the transient reactance of the machines are included along with normal Y_{BUS}. P_{Li} and Q_{Li} are the real and reactive powers loads, respectively, at the ith bus [10], [13].

C. Quantification of TS and Its Implication

The state variables for the power system (described in the previous subsection) are the generator rotor angle (δ) and rotor speed deviation $(\Delta\omega_r)$. Sensitivity of these state variables with respect to any parameter λ can be computed as in (3). For angular stability study, relative rotor angles are considered instead of individual rotor angles. Generally one of the generators with large inertia (say, the jth one here) is considered as the reference, and the relative rotor angle of the ith machine is found as $\delta_{ij} = \delta_i - \delta_j$ [10], [14]. The sensitivity of δ_{ij} with respect to λ is computed as

$$\frac{\partial \delta_{ij}}{\partial \lambda} = \frac{\partial \delta_i}{\partial \lambda} - \frac{\partial \delta_j}{\partial \lambda}. \tag{8}$$

However, individual speed deviation is considered here (and not relative speed deviation) because of the nonzero damping.

The center of inertia (COI) can also be used as reference instead of one of the machines. The COI angle and speed are given by

$$\delta_{\text{COI}} = \frac{1}{M_T} \sum_{i=1}^{m} M_i \delta_i \tag{9}$$

$$\omega_{r_{\text{COI}}} = \frac{1}{M_T} \sum_{i=1}^{m} M_i \omega_{r_i} \tag{10}$$

where

$$M_T = \sum_{i=1}^{m} M_i \tag{11}$$

and

$$M_i = \frac{2H_i}{\omega_s}. \tag{12}$$

The COI referenced rotor angles and speeds are given by

$$\bar{\delta}_i = \delta_i - \delta_{\text{COI}} \tag{13}$$

$$\bar{\omega}_{r_i} = \omega_{r_i} - \omega_{r_{\text{COI}}}. \tag{14}$$

Equations (4) and (5) can be modified using (13) and (14). Then proceeding as before, the rotor angles and speeds in the COI

reference frame can be obtained. However, relative rotor angle formulation involves lesser analytical work.

Trajectory sensitivities give us information about the effect of change of parameter on individual state variables and hence on the generators (to which the particular state variable correspond) of the system. However, to know the overall system condition, we need to sum up all these information and develop a suitable metric. To achieve this goal, the norm of these sensitivities of δ_{ij} and $\Delta\omega_r$ are calculated. Other metrics can also be developed including the TEF itself without computing UEP as reported in [4]. The sensitivity norm for an m machine system is given by (15). It was observed that the contribution of the frequency deviations to the norm is very negligible. However, it is retained here to reflect the general theory of TS. Then a new term η (ETA) is introduced [4], which is defined as in

$$S_N(t) = \sqrt{\sum_{i=1}^{m}\left[\left(\frac{\partial\delta_{ij}}{\partial\lambda}\right)^2 + \left(\frac{\partial\Delta\omega_{r_i}}{\partial\lambda}\right)^2\right]} \tag{15}$$

$$\eta = 1/\max(S_N(t)). \tag{16}$$

As the system moves toward instability, the oscillation in TS will be more, resulting in larger values of S_N(t). This will result in the smaller values of η. Ideally, η should be zero at the point of instability. Therefore, the value of η gives us an indication of the distance from instability. In this paper, TS with respect to fault clearing time and the corresponding η has been used for assessing the relative stability margins of the system.

III. Effects of Series Compensation on Transient Stability

The study systems considered are the WSCC three-machine nine-bus system shown in Fig. 1 [10] and the IEEE 16-machine 68-bus system [11] shown in Fig. 2.

A. Variation of η With Fault Clearing Time

Let us first investigate the effect of variation of fault clearing time ($t_{\rm cl}$) on TS and η in the uncompensated system. A three-phase fault is simulated in one of the lines of the nine-bus system. The simulation is done in three phases. To start with, the pre-fault system is run for a small time. Then a symmetrical fault is applied at one end of a line. Simulation of the faulted condition continues until the line is disconnected from the buses at both of the ends of the faulted line after a time $t_{\rm cl}$ s. Then the post-fault system is simulated for a longer time (say, 10 s) to observe the nature of the transients. We start with $t_{\rm cl} = 0.1$ s (which is six cycles for a 60-Hz system) and compute the TS and η. Then the $t_{\rm cl}$ is increased in steps to observe the change in TS in the post-fault phase as represented by η. The results are given in Table I. As expected, an increase in $t_{\rm cl}$ reduces the value of η, indicating a reduction in transient stability margin. Also it can be seen that η is minimum for a fault in line 7–8 (at any particular value of $t_{\rm cl}$), indicating proximity to instability. On the other hand, η is much higher for fault in line 4–6, 5–7, or 6–9 (at any particular value of $t_{\rm cl}$), indicating a more stable system. This can be verified from the results of PSCAD/EMTDC simulation. Plots of relative machine angles delta-31 ($\delta_3 - \delta_1$) are shown in Fig. 3(a) for

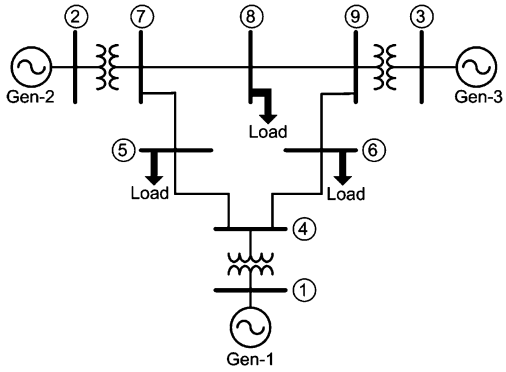

Fig. 1. Single line diagram of the WSCC nine-bus system.

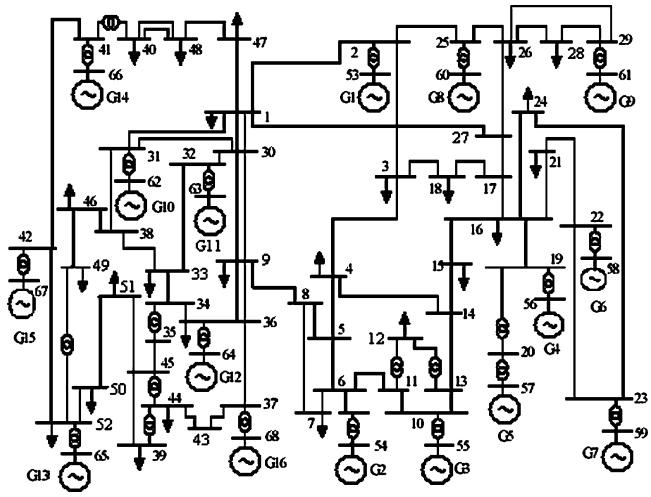

Fig. 2. Single line diagram of the 16-machine 68-bus system.

TABLE I
Variation of η With Fault Clearing Time

9-bus system			68-bus system		
Fault applied in line	Fault clearing time		Fault applied in line	Fault clearing time	
	0.10s	0.15s		0.05s	0.10s
	η	η		η	η
6-4	0.2292	0.2018	16-15	0.0567	0.0103
6-9	0.2269	0.2004	26-25	0.0832	0.0167
5-7	0.2201	0.1951	24-23	0.0703	0.0297
8-9	0.1625	0.0965	3-2	0.0797	0.0404
8-7	0.1269	0.0434	5-6	0.0952	0.0620
5-4	0.2261*	0.1994*	11-10	0.1019	0.0771
			9-8	0.1218	0.1092
			1-47	0.1606	0.1314
			33-34	0.1704	0.1341
			43-44	0.1443	0.1412

* For fault in line 5-4, there is some convergence problem with constant PQ load. Hence, load is considered to be constant impedance in this case

faults ($t_{\rm cl} = 0.15$s) in lines 7–8 and 6–9. Larger oscillation in case of fault in 7–8 also indicates proximity to instability and supports the corresponding lower value of η. Therefore, it can be said that η gives a fair idea about the transient stability margin of the system.

The same study is carried out in the 68-bus system. The initial $t_{\rm cl}$ is 0.05 s here, and it is increased in steps as before. These results are also given in Table I. The value of η is found to vary

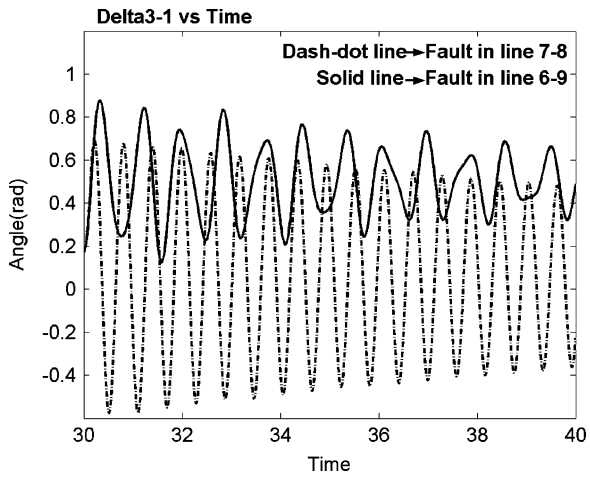

(a)

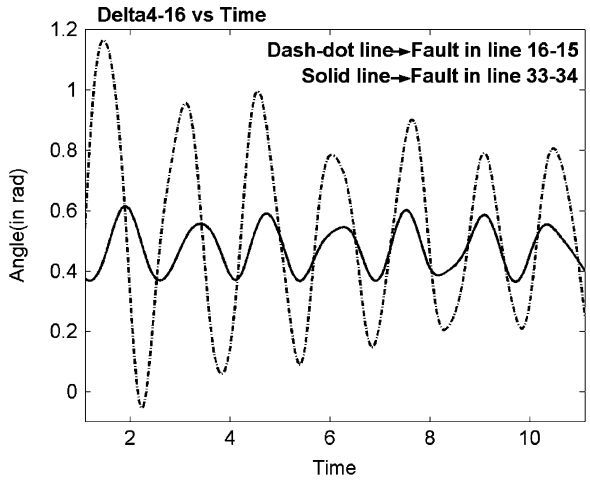

(b)

Fig. 3. (a) Response of relative rotor angle delta3-1 for fault in line 7–8 and 6–9. (b) Relative machine angles Delta 4–16 for fault in 16-15 and 33–34.

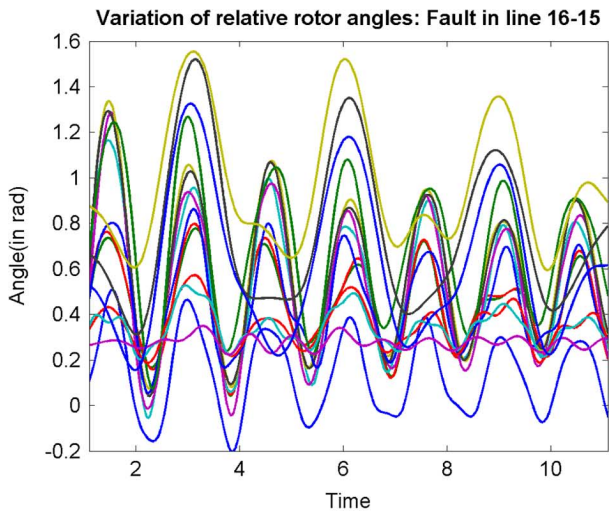

(a)

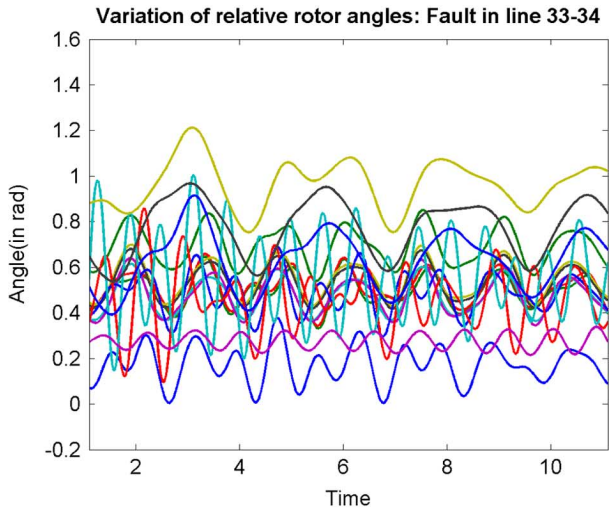

(b)

Fig. 4. Relative rotor angles of all the machines for fault in (a) line 16-15 and (b) line 33–34.

widely for fault in different lines, indicating different stability margins. For example, η is very low (0.0103) for a fault in line 16-15. Also for faults in lines 26-25, 24-23, and 3-2, the values of η are 0.0167, 0.297, and 0.0404, respectively. These indicate that the system comes very close to instability for fault in these lines. However, for fault in line 1–47, 33–34, or 43–44, the η values are much higher (0.1314, 0.1341, and 0.1412, respectively), indicating comparatively stable system. These results can be verified from Fig. 3(b), which shows the post-fault excursions of relative rotor angles delta4-16 for fault in line 16–15 and line 33–34. It can be seen that the oscillation in relative rotor angle is much more in case of fault in line 16-15, indicating a less stable system. For further verification, the relative rotor angles of all the machines are plotted in the same figure. Responses of all relative rotor angles for a fault in line 16-15 are shown in Fig. 4(a), and those for a fault in line 33-34 are shown in Fig. 4(b). It is clear from the figures that the oscillations are much more in the first case.

As described in Section II-C rotor angles referred to COI frame can also be used instead of referring them to the rotor angle of one reference machine. This is also done here, and the η values for a few cases are given in Table II. It can be seen that the results are similar to the corresponding results shown in Table I, e.g., out of the three fault locations in 68-bus system, η is smallest for a fault in line 16-15 and largest for fault in 33–34. These are in accordance with Table I. Similarly, in case of the nine-bus system, the highest and lowest η (out of the three cases shown) are for fault in lines 6-4 and 8–7, respectively. This also matches with Table I.

These can be verified by plots of the rotor angles referred to COI frame. For comparison with Fig. 3(b), Delta 4 is plotted

TABLE II
VARIATION OF η WITH FAULT CLEARING TIME-COI REFERENCE

9-bus system			68-bus system	
Fault applied in line	Clearing time 0.15s		Fault applied in line	Clearing time 0.10s
	η			η
6-4	0.2959		16-15	0.0123
8-9	0.1168		3-2	0.0403
8-7	0.0488		33-34	0.1396

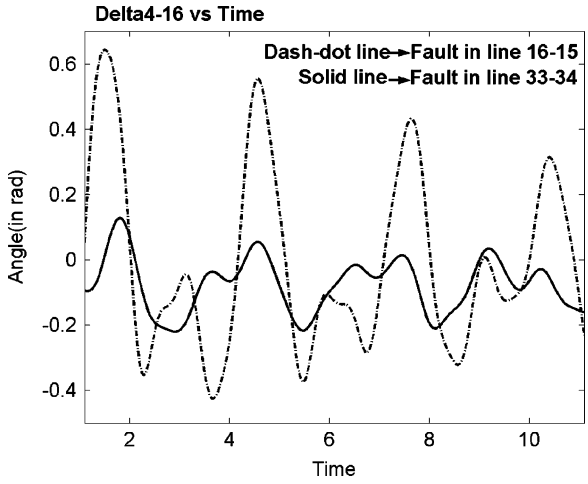

(a)

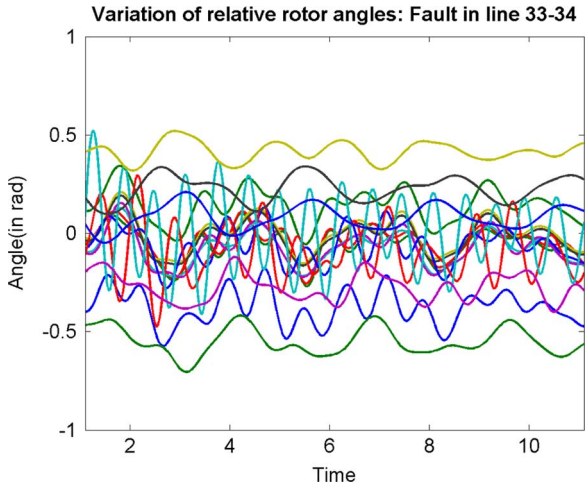

(b)

Fig. 5. (a) Delta 4–16 in COI reference frame for fault in lines 16-15 and 33–34. (b) Relative rotor angles of all the machines for fault in line 33–34.

in Fig. 5(a) for the same two cases, i.e., fault in line 16-15 and line 33–34. It is to be noted that the plots in the two figures are different in terms of shape and magnitude because of the use of different reference frames in the calculation of the relative rotor angles. However, these figures are shown here to verify the fact that both of them carry the same information about relative stability of the system on the occurrence of fault at two different locations. Therefore, the comparison between the oscillations of the relative rotor angles in the two cases (fault in line 16-15 and 33–34) is the relevant factor here. It can clearly be observed in both the figures that the relative rotor angle oscillates much more in case of a fault in line 16-15 than in case of a fault in 33–34. This implies that the former is more prone to instability than the latter. Therefore, in spite of different shape and magnitude, both of the figures tell us the same information about relative stability condition. Plots of the rotor angles of all the machines in COI reference frame are shown in Fig 5(b) for the case of fault in line

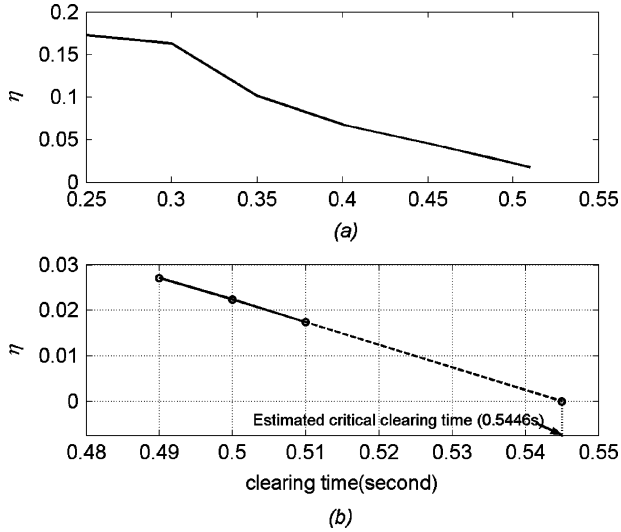

Fig. 6. Variation of η with clearing time and estimation of $t_{\rm cr}$: Fault in line 6–9.

TABLE III
ESTIMATION OF $t_{\rm cr}$ USING η

System	Fault in line	Estimated t_{cr}	Actual t_{cr}
9-bus system	6-9	0.5446	0.5450
	6-4	0.6090	0.6100
	5-7	0.4444	0.4450
68-bus system	11-10	0.2256	0.2250

33–34. It can be observed that the plots are very much similar to the case with one machine taken as reference [see Fig. 4(b)].

TSA and η can also be used to estimate the critical clearing time $(t_{\rm cr})$ as in [4]. Fig. 6(a) shows the variation of η with clearing time for a fault in line 6–9 of the nine-bus system. Simulation is done with system load as constant PQ, and it is converted to constant impedance when problems with convergence are encountered (e.g., at larger clearing time). As discussed before, η decreases with increase of clearing time. At the point of instability, η is expected to be zero. The corresponding clearing time is $t_{\rm cr}$. It is apparent from the figure that the plot is almost linear near $t_{\rm cr}$. Therefore, if we take two points in this linear zone and extrapolate the line connecting them to intersect $\eta = 0$ line, we get the estimated value of $t_{\rm cr}$, as is done in Fig. 6(b). Power system operators have a fair idea about the approximate range of $t_{\rm cr}$. With that knowledge, one can easily find an estimate of $t_{\rm cr}$ using the above method.

The estimated $t_{\rm cr}$ and the corresponding actual values found from simulation for a few cases are given in Table III. It is clear that the estimated and actual values match quite closely.

B. Series Compensation: Modeling of TCSC

Series compensation is provided here by putting a TCSC in one of the lines of the power system. The TCSC model is given in Fig. 7. The TCSC capacitor voltage (v_S), inductor current (i_L) relationship is also shown in this figure where α is the firing angle of the thyristors, measured from the zero crossing of the capacitor voltage. The overall reactance X_C of the TCSC is given in terms of the firing angle α as [15]

$$X_C = \beta_1(X_{FC} + \beta_2) - \beta_4\beta_5 - X_{FC} \qquad (17)$$

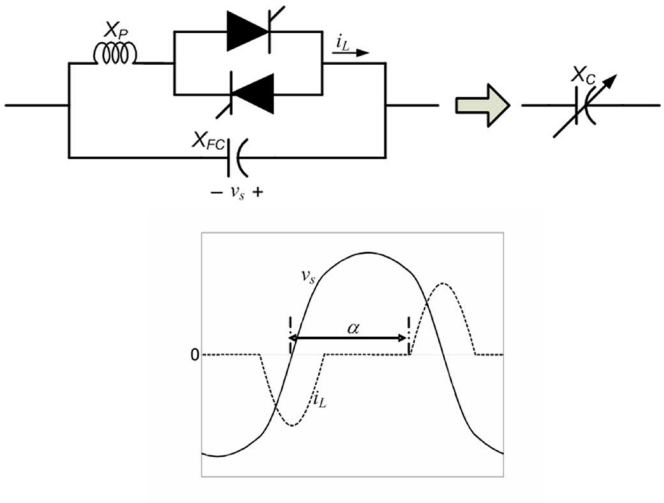

Fig. 7. TCSC circuit and its equivalent and voltage-current relationship.

where

$$\beta_1 = \frac{2(\pi-\alpha)+\sin 2(\pi-\alpha)}{\pi}, \beta_2 = \frac{X_{FC}X_P}{X_{FC}-X_P}$$
$$\beta_3 = \sqrt{\frac{X_{FC}}{X_P}}$$
$$\beta_4 = \beta_3 \tan[\beta_3(\pi-\alpha)] - \tan(\pi-\alpha)$$
$$\beta_5 = \frac{4\beta_2^2 \cos^2(\pi-\alpha)}{\pi X_P}.$$

Here C is the fundamental frequency capacitance of the TCSC and is equal to $1/(\omega_s X_C)$. It is to be noted that in this paper, the TCSC is operated only in the capacitive mode. The capacitive reactance X_{FC} of the TCSC is chosen to be half of the reactance of the line in which the TCSC is placed, and the TCR reactance X_P is chosen to be one third of X_{FC}. The net reactance of the line is calculated as the difference between the line reactance and the TCSC reactance.

C. Effect of Compensation With TCSC

The TCSC is now placed in different lines of the system, one at a time. The firing angle of the TCSC is chosen between 140° and 180° so that the TCSC is in the capacitive mode. The η value changes for different locations and firing angles of the TCSC, indicating changes in the transient stability condition. The variation of η for different locations of fault and TCSC in the nine-bus system with firing angles of 160° and 145° are shown in Table IV. A firing angle of 145° is very close to resonance, and a firing angle of 160° gives a stable TCSC operation. Therefore, study at these two operating conditions provides an overall trend of the system behavior. The values of η for the uncompensated system (termed as η_0) are also given in the first column of the table for comparison. In all these cases, t_{cl} is taken to be 0.15 s.

Next, the effect of TCSC placement is studied in the 68-bus system as well. Five of the cases given in Table I are chosen for study, which are fault in line 3-2, 26-25, 1-47, 11-10, and 33–34. TCSC is placed in several locations for each of these five cases with α set at 160°, and the changes in η are observed. The results are given in Table V. The η_0 values are also given for comparison. The t_{cl} is assumed as 0.1 s in all the cases.

TABLE IV
VARIATION OF η WITH COMPENSATION BY TCSC, NINE-BUS SYSTEM

Fault in line, η_0	α	With TCSC connected between buses				
		6-4	5-7	6-9	8-7	8-9
6-4, *0.2018*	160°	--	**0.2411**	0.2353	0.2039	0.2017
	145°	--	0.2665	**0.3074**	0.2049	0.2012
5-7, *0.1951*	160°	0.2058	--	**0.2302**	0.1963	0.1968
	145°	0.2113	--	**0.2506**	0.1964	0.1976
6-9, *0.2004*	160°	0.1514	**0.2409**	--	0.2023	0.2005
	145°	0.0915	**0.2666**	--	0.2033	0.2001
8-7, *0.0434*	160°	0.0518	**0.0551**	0.0471	--	0.0365
	145°	**0.0548**	0.0542	0.0449	--	0.0341
8-9, *0.0965*	160°	0.0947	**0.1214**	0.1019	0.0735	--
	145°	0.0915	**0.1242**	0.1007	0.0647	--

TABLE V
VARIATION OF η WITH COMPENSATION BY TCSC, 68-BUS SYSTEM

Fault in 3-2		Fault in 26-25		Fault in 11-10	
η_0=0.0404		η_0=0.0167		η_0=0.0771	
TCSC in line	η	TCSC In line	η	TCSC In line	η
3-4	0.0314	28-29	0.0260	10-13	0.0759
3-18	0.0337	26-27	0.0312	13-14	0.0715
18-17	0.0369	26-28	0.0263	6-11	0.0672
2-25	0.0411	**26-29**	**0.0352**	5-6	0.0763
1-27	0.0451	17-27	0.0322	26-29	0.0767
1-2	0.0495	1-2	0.0157	1-2	0.0847
8-9	0.0664	8-9	0.0160	**8-9**	**0.0933**
50-51	0.0607	50-51	0.0165	50-51	0.0888
50-52	**0.0688**	50-52	0.0164	50-52	0.0886
49-52	0.0628	49-52	0.0162	49-52	0.0885

Fault in 33-34		Fault in 1-47	
η_0=0.1341		η_0=0.1314	
TCSC in line	η	TCSC In line	η
32-33	0.1178	1-30	0.1141
33-38	0.1239	1-31	0.1279
34-36	0.1290	40-48	0.1272
30-32	0.1399	47-48	0.1309
34-35	0.1351	46-49	0.1422
1-2	0.1292	1-2	0.1094
8-9	0.1236	8-9	0.1219
50-51	0.1451	50-51	0.1621
50-52	0.1453	50-52	0.1631
49-52	**0.1457**	**49-52**	**0.1661**

The following observations can be made from the results given in Tables IV and V.

1) The best possible location of TCSC varies with fault location: In the nine-bus system, for a fault in line 5-7, the transient stability of the system improves the most when the TCSC is placed in line 6-9. Therefore, it is termed as the best possible location. However, this best possible location changes to line 5-7 when the fault takes place in one of the lines 8-9, or 6-9. When the fault is in 6-4 or 8-7, the best possible location is dependent on the value of α.
2) Improvement in stability margin due to TCSC varies: The system stability conditions are poor for faults in lines 7-8 or 8-9. Compensation with TCSC does not improve the

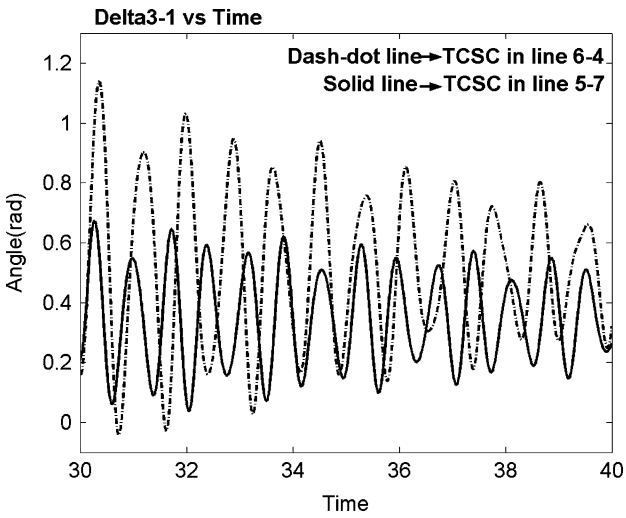

Fig. 8. Response of delta3-1 for fault in line 6-9 with TCSC in line 6-4 and 5-7.

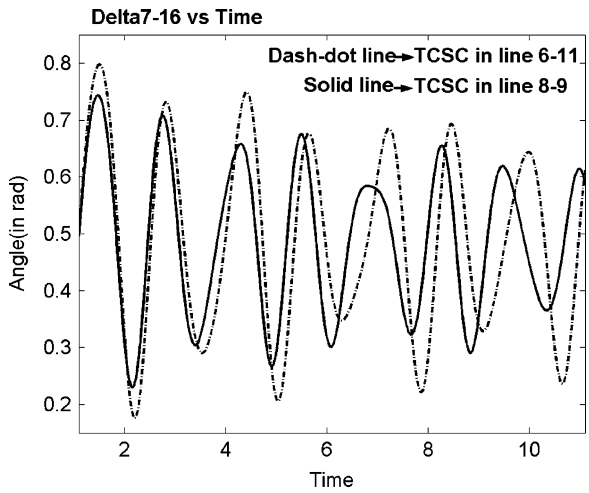

Fig. 9. Plot of delta7-16 for TCSC in line 6-11 and 8-9 with fault in line 11-10.

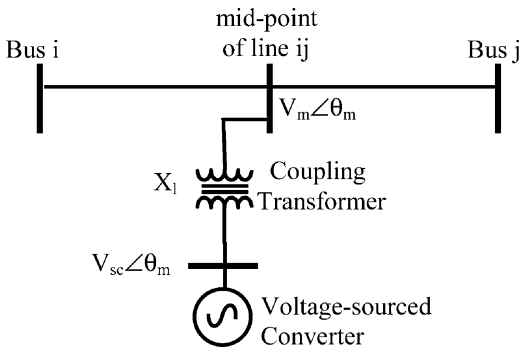

Fig. 10. Representation of STATCOM.

condition by a large margin, but for fault in other lines, the effect of TCSC is considerable.

3) Assessment of stability margin for different TCSC locations is necessary: TCSC causes improvement of stability in most of the cases. However, it is to be noted that there are cases when system stability may even deteriorate with the placement of TCSC in some of the lines. For example, for a fault in line 6-9, the value of η in uncompensated system is 0.2004. It falls to 0.0915 when a TCSC is placed in line 6-4 and the firing angle is set at 145°. Therefore, it is important to judge the system stability condition with different TCSC locations and firing angles for operating in the stable operating range.
4) Trends are similar in the 68-bus system also: The effect of TCSC on system stability margin varies depending on the locations of fault and TCSC in the 68-bus system also. It can be seen from the results that with fault in line 3-2, the placement of TCSC in line 50-52 improves the system stability as indicated by the increase in η value from 0.0404 (base case) to 0.0688. On the other hand, placement of the TCSC in line 3-4 drags the system more near to instability as indicated by the fall in the value of η to 0.0314. Similarly, for a fault in lines 26-25, 11-10, 33–34, and 1-47, the system stability condition improves most with the TCSC in lines 26-29, 8-9, and 49-52, respectively, out of the ten lines considered in each case.
5) Distance of TCSC from fault is not the deciding factor: Another important point is that placing the TCSC in lines adjacent to the faulty line is not necessarily beneficial. For example, in case of a fault in line 11-10, the stability margin deteriorates with the TCSC in 6-11, one of the adjacent lines, whereas it improves with the TCSC in 8-9, which is not in the vicinity of the faulty line. Similar is the case for fault in line 3-2, where 3-4 is an adjacent line, whereas 50-52 is far away.

The simulation results to verify the changes in system stability condition with placement of TCSC are shown in Figs. 8 and 9. A fault of duration 0.15 s is simulated in line 6-9 of the nine-bus system. The responses of relative machine angle delta3-1 are shown in Fig. 8 for two cases: 1) the TCSC placed in line 4-6 and 2) TCSC placed in line 5-7. The firing angle of TCSC is 160° in both of the cases. It is clear that the maximum peak of the response is much lower in case of TCSC in line 5-7, which indicates a higher transient stability margin. This is in accordance with the higher value of η for the TCSC in line 5-7 than in line 4-6 in the corresponding cases in Table IV. Similarly for a fault in line 11-10 of the 68-bus system (with $t_{cl} = 0.1$s), the plots of delta7-16 are shown in Fig. 9 for 1) TCSC placed in line 6-11 and 2) line 8-9. It is clear from the figure that the oscillations reduce when the TCSC is placed in line 8-9, indicating a more stable system. The stability margin increases further when the firing angle of the TCSC is changed to 145° as indicated by an increase in the value of η to 0.0993.

IV. Effects of Shunt Compensation on Transient Stability of The System

Next, the effect of shunt compensation is studied. Shunt compensation is provided by connecting a STATCOM at the midpoint of one of the lines of the system.

A. Modeling of STATCOM

The STATCOM is modeled by a voltage source connected to the power system through a coupling transformer. The voltage of the source is the output of a voltage-sourced converter (VSC) realizing the STATCOM. As shown in Fig. 10, the connection

is assumed at the midpoint of the transmission line. The phase angle of the source voltage is the same as that of the midpoint voltage. This ensures that there is exchange of only reactive power and no real power between the STATCOM and the ac system [16], [17]. The expressions for the current flowing from the STATCOM to the system and the reactive power injection are given as

$$I = \frac{(V_{sc} - V_m)\angle\theta_m}{jX_l} \tag{18}$$

$$Q = V_m^2 \cdot \frac{(V_{SC}/V_m - 1)}{X_l} \tag{19}$$

where V_{sc} is the magnitude of the voltage of the voltage-sourced converter and V_m is the magnitude of the voltage at the midpoint of the line, θ_m is the phase angle of the mid-point voltage, and X_l is the leakage reactance of the coupling transformer. The value of V_{sc} determines the direction (and hence nature) of the reactive power flow. If it is higher than the magnitude of the line midpoint voltage (V_m), then reactive power is injected to the ac system, whereas if the line midpoint voltage magnitude is higher, then reactive power will be drawn from the ac system. In this paper, only the reactive power injection mode of operation (i.e., $V_{sc}V_m$) is considered. The leakage reactance of the coupling transformer is taken to be 0.1 p.u.

A constant value of source voltage magnitude may result in a very high value of current drawn from the STATCOM (I_{sc}), especially during fault conditions. To avoid this, a maximum limit, denoted by $I_{\max}$, is set for the STATCOM current. In a practical system, this current limit is decided by the rating of the STATCOM. Once the current reaches the limit $I_{\max}$, STATCOM behaves like a constant current source. To incorporate this feature in the simulation, V_{sc} is kept constant at the pre-specified value (denoted by V_{sc0}) when $I_{sc} \leq I_{\max}$. However, whenever the value of I_{sc} exceeds $I_{\max}$, the value of V_{sc} is adjusted such that I_{sc} becomes equal to $I_{\max}$.

B. Effect of Compensation With STATCOM

Similar to the previous case, a three-phase fault is simulated in one of the lines with $t_{\rm cl} = 0.15$ s for the nine-bus system and $t_{\rm cl} = 0.1$ s for the 68-bus system. The STATCOM is connected to the midpoint of one of the lines. To ensure the reactive power injection mode of operation, the magnitude of the voltage of the STATCOM (V_{sc}) is set at a value higher than the magnitudes of the pre-fault line midpoint voltage. The magnitudes of pre-fault midpoint voltages of different lines of the nine-bus system are found to range between 1.009 and 1.025 p.u. Therefore, the specified STATCOM voltage magnitude, V_{sc0}, is taken to be 1.05 p.u. or more. The value of $I_{\max}$ is set at 0.8 p.u. when the V_{sc0} is 1.05. Similarly for $V_{sc0} = 1.10$ p.u., $I_{\max}$ is set at 1.0 p.u. This value of $I_{\max}$ is chosen such that the STATCOM current does not hit the limit in steady state. The variation in η and hence the transient stability condition is studied with the STATCOM placed in different lines. The effect of changes in the amounts of compensation on the system stability is also observed by changing the value of $I_{\max}$. The results are given in Table VI. The values of η_0 are given for comparison.

Similarly, the results for the 68-bus system are given in Table VII. The same five cases studied in Section III-C (fault in 3-2, 26-25, 11-10, 33–34, and 1-47) are considered here also. STATCOM is placed in several locations with $V_{sc0} = 1.10$ for each of the five cases, and the changes in η are observed. The corresponding values of $I_{\max}$ are shown in the table.

TABLE VI
VARIATION OF η FOR COMPENSATION WITH STATCOM, NINE-BUS SYSTEM

Fault in line, base η	I_{max}	With STATCOM connected between buses				
		6-4	5-7	6-9	8-7	8-9
6-4, *0.2018*	0.80	--	0.2330	0.2299	0.2480	**0.2527**
	1.00	--	0.2409	0.2392	0.2597	**0.2656**
5-7, *0.1951*	0.80	0.2060	--	0.2279	0.2386	**0.2399**
	1.00	0.2081	--	0.2350	0.2495	**0.2507**
6-9, *0.2004*	0.80	0.2012	0.2324	--	0.2467	**0.2507**
	1.00	0.2010	0.2403	--	0.2585	**0.2635**
8-7, *0.0434*	0.80	0.0953	0.0754	**0.1327**	--	0.1286
	1.00	0.1008	0.0778	**0.1446**	--	0.1338
8-9, *0.0965*	0.80	0.1430	**0.1476**	0.1442	0.1452	--
	1.00	0.1432	**0.1486**	0.1452	0.1453	--

TABLE VII
VARIATION OF η WITH COMPENSATION BY STATCOM, 68-BUS SYSTEM

Fault in 3-2, I_{max}=1.50		Fault in 26-25, I_{max}=1.00		Fault in 11-10, I_{max}=1.50	
η_0=0.0404		η_0=0.0167		η_0=0.0771	
Statcom in line	η	Statcom in line	η	Statcom in line	η
16-17	0.0506	**28-29**	**0.0550**	**14-15**	**0.0907**
15-16	**0.0511**	26-29	0.0513	13-14	0.0902
17-18	0.0501	26-28	0.0502	15-16	0.0900
16-21	0.0506	26-27	0.0423	10-13	0.0890
3-4	0.0499	17-27	0.0351	16-24	0.0893
1-2	0.0454	34-35	0.0155	6-11	0.0901

Fault in 33-34, I_{max}=1.40		Fault in 1-47, I_{max}=1.00	
η_0=0.1341		η_0=0.1314	
Statcom in line	η	Statcom in line	η
30-32	**0.1484**	30-32	0.1408
30-31	0.1472	1-30	0.1399
34-36	0.1433	1-31	0.1403
31-38	0.1471	1-27	0.1366
32-33	0.1458	1-2	0.1374
33-38	0.1462	**30-31**	**0.1410**

The observations from the tables are listed below.

1) Best possible location of the STATCOM varies: The best possible location for STATCOM placement is found to vary with the changes in fault location. For example, placing the STATCOM in line 8-9 of the nine-bus system results in the maximum value of η when the fault is in line 6-4, 5-7, or 6-9. However, for a fault in line 8-7, the best possible location is line 6-9.
2) STATCOM may also cause deterioration of stability: Arbitrary placement of the STATCOM is not always beneficial, e.g., stability margin increases with placement of STATCOM in line 28-29 of the 68-bus system for a fault in line 26-25, whereas stability condition deteriorates with placement of STATCOM in line 34-35 for a fault in 26-25 as indicated by the decrease in η.
3) Increase in $I_{\max}$ does not ensure improvement in stability in all cases: Increase in $I_{\max}$ improves the stability condition in most of the cases. However, in some cases, it has a

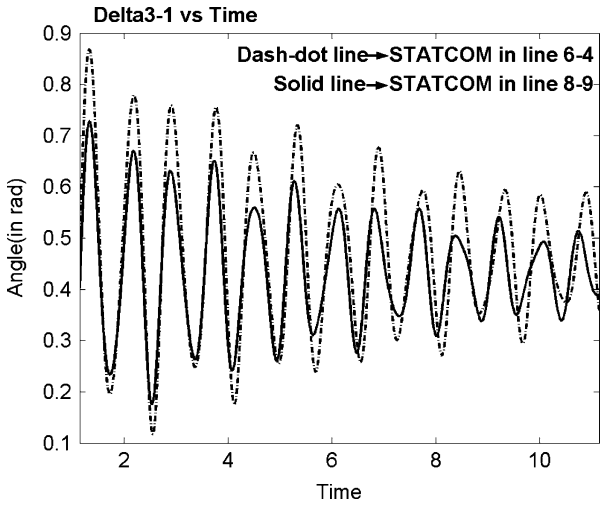

Fig. 11. Response of relative rotor angle delta 3-1 to a fault in line 6-9 with STATCOM in line 4-6 and 8-9.

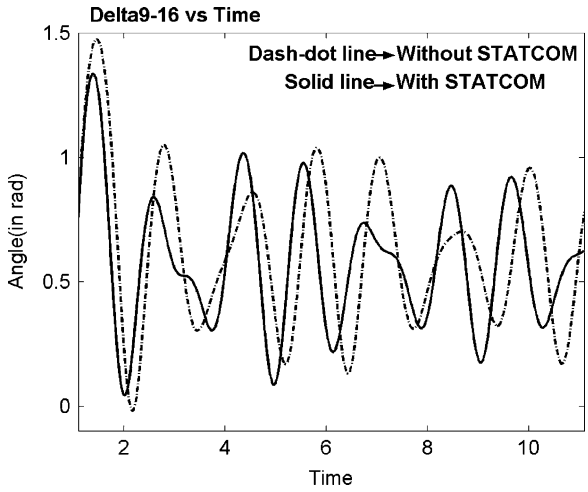

Fig. 12. Response of relative machine angles Delta 9-16 for fault in line 26-25, without STATCOM, and with STATCOM in line 28-29.

reverse effect. For example, for a fault in line 6-9 and the STATCOM placed at 6-4, η decreases as the value of $I_{\max}$ is increased from 0.8 to 1.0 p.u.

Fig. 11 shows the responses of relative rotor angle delta-31 to a fault in line 6-9 of the nine-bus system (with $t_{\rm cl} = 0.15$ s) for two different locations of the STATCOM, line 4-6 and line 8-9 ($I_{\max} = 1.0$ in both cases). The oscillation of the response is much more in case of the compensator in line 6-4, indicating a poor stability condition. It can be checked from Table VI that the corresponding value of η is also less. Similarly, Fig. 12 shows the response of relative machine angle delta9-16 for a fault in line 26-25 of the 68-bus system for 1) system without STATCOM and 2) STATCOM located in 28-29. Larger oscillation in the former case supports the result of Table VII.

The discussion in Sections III and IV can be summarized with the following words.

$\surd$ It is found that the best possible location of the FACTS devices (in terms of transient stability improvement) is not fixed for a particular system; rather it varies depending on the location of the fault.

TABLE VIII
COMPARISON OF EFFECTS OF INDIVIDUAL FACTS DEVICES AND THEIR COMBINATION ON η, FIRING ANGLE $= 145°$ AND $I_{\max} = 1.10$

Fault in line	Without Comp	Compensation by TCSC only		Compensation by STATCOM		Combined effect
		In line	η	In line	η	
6-4	0.2018	6-9	0.3074	8-9	0.2656	0.5698
6-9	0.2004	5-7	0.2666	8-9	0.2635	0.3673

$\surd$ However, the system operators and planners generally do have information regarding fault prone lines, and therefore, this TSA-based method can be used in such cases to find out the best possible location for the FACTS device. Also this method itself can help in identifying the locations where a fault will cause maximum damage to the system.

$\surd$ Though the FACTS devices cause improvement of system stability margin in the majority of the cases, it may effect deterioration for some combinations of fault and FACTS device locations.

$\surd$ The increase of compensation by change of α of the TCSC or $I_{\max}$ of the STATCOM may cause improvement or deterioration in stability, depending upon the locations of compensators. TSA can help in this assessment.

It is quite clear that before compensating a power system with FACTS devices to improve transient stability, we need to assess the system stability conditions for different locations of the fault and the compensator and also with different amounts of compensation. The above studies show that TS and η can help in making that assessment.

V. SIMULTANEOUS APPLICATION OF SERIES AND SHUNT COMPENSATION

The TCSC and STATCOM are now placed in an ac system simultaneously at different places. The effect of placement of the two compensators at various locations on the transient stability of the system is studied. A comparison of the individual effects of the TCSC and the STATCOM with those for the two devices applied simultaneously is carried out.

A. Comparison of Individual and Combined Effects

If both TCSC and STATCOM cause improvement in stability individually when placed in some locations, then their simultaneous placement in those particular locations results in larger improvement of stability in comparison to their individual effects. Examples of this are shown in Table VIII. For a fault in line 6-4, putting a TCSC alone in line 6-9 with $\alpha = 145°$ improves stability condition (η increases from the base value of 0.2018 to 0.3074) and putting the STATCOM alone in line 8-9 with $I_{\max} = 1.0$ also improves stability (η increases to 0.2656). When the two devices are placed simultaneously in these two locations, the stability condition of the system improves further (η increases to 0.5698). Similar is the case of fault in line 6-9. Here TCSC in 5-7 and STATCOM in 8-9 cause improvement in stability individually. On simultaneous placement of the two devices at these particular locations, the improvement of stability is more than the individual effects. This is verified by the plots of relative rotor angle delta 2-1 (see Fig. 13) for the three cases mentioned above. We can see that the oscillations are much less

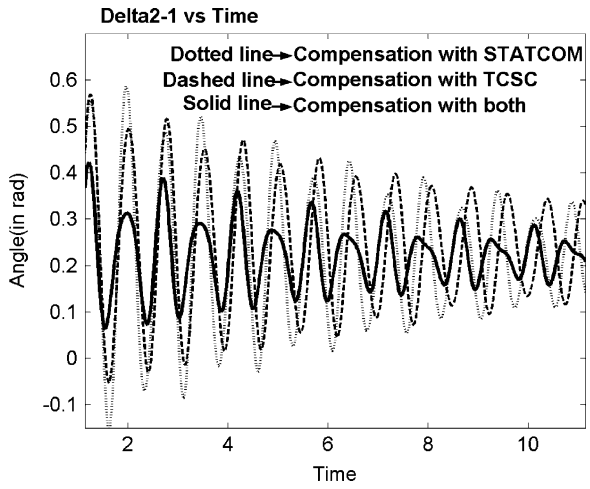

Fig. 13. Relative rotor angle delta 2-1 with a fault in line 6-4 for system with TCSC alone (in 6-9), STATCOM alone (in 8-9), and the two together.

TABLE IX
COMPARISON OF BEST LOCATIONS FOR INDIVIDUAL AND SIMULTANEOUS PLACEMENT OF FACTS DEVICES

System α and I_{max}	Fault in line	Best location for individual placement of compensator		Best location for simultaneous placement of compensator	
		TCSC	STATCOM	TCSC	STATCOM
9-bus, 160°, 1.00	6-9	5-7	8-9	5-7	8-9
	5-7	6-9	8-9	6-9	8-7
	6-4	5-7	8-9	6-9	8-9
68-bus, 160°, 1.50	26-25	26-29	28-29	26-29	28-29
	11-10	8-9	14-15	8-9	13-14

for the case of simultaneous compensation, which indicate a more stable system.

However, the best possible location of the compensators for simultaneous placement may be different from those for individual placement. A comparison of best locations of compensators for individual and simultaneous placement is shown in Table IX. The fault clearing time is taken as 0.15 s for the nine-bus and 0.10 s for the 68-bus system. The firing angle of TCSC (α) and STATCOM current magnitude limit $(I_{\max})$ are mentioned in the first column. It can be seen from the table that for a fault in line 6-9 in the nine-bus system (with $\alpha = 160°$ and $I_{\max} = 1.0$), the individual best locations are the same as the best locations for simultaneous placement of the devices (line 5-7 for TCSC and line 8-9 for STATCOM). However, for a fault in line 5-7, the best locations for individual (line 6-9 for TCSC and line 8-9 for STATCOM) and simultaneous placement (line 6-9 for TCSC and line 8-7 for STATCOM) are different. Similarly, in the 68-bus system, also the best locations differ for a fault in line 11-10. The best location for TCSC and STATCOM are lines 8-9 and 14-15, respectively, for individual placement. However, when the devices are placed simultaneously, the best location combination is 8-9 for TCSC and 13-14 for STATCOM.

B. Effect of Change in Operating Condition: Overloaded System

The study up to this point is carried out with the system loads at their nominal values. Let us investigate the effects of compensation by TCSC and STATCOM in a stressed system. Overload may be a possible reason of stress on the system. Therefore, studies similar to that described in Sections III, IV, and V-A are carried out for the system with increased load in one load bus at a time. All of the three generators share this extra load in the ratio of their generation at nominal load. Tables X and XI show a comparison of effects of compensation by FACTS devices on the nine-bus system at nominal loading condition and overloaded condition. The load is increased by 20% in one of the three load buses (bus 5, 6, and 8) at a time, and compensation is provided by a TCSC and a STATCOM simultaneously at two different locations. A comparison of best possible locations of the FACTS devices (in terms of improvement of stability margin) in nominally loaded and overloaded system is shown in Table X. The value of α is 145° and $I_{\max}$ is 1.0. Table XI shows the variation of η for different locations of TCSC and STATCOM when there is a fault in line 8-9. The value of α is 160° and $I_{\max}$ is 1.0. Twenty percent overloading is considered at bus 6. The value of $t_{\rm cl}$ is taken as 0.15 s.

TABLE X
COMPARISON OF BEST LOCATIONS OF TCSC AND STATCOM IN SYSTEM WITH NOMINAL LOAD AND OVERLOAD

Fault in line	Loading Condition	TCSC In line	STATCOM In line
8-7	Nominal	5-7	6-9
	Overload at bus 6	5-7	6-9
	Overload at bus 8	5-7	8-9

TABLE XI
COMPARISON OF EFFECTS OF COMPENSATION ON η IN SYSTEMS WITH NOMINAL LOAD AND OVERLOAD; FAULT IN LINE 8-9°

TCSC in line	Loading Condition	STATCOM in line				
		4-5	6-4	5-7	6-9	8-7
5-7	nominal	0.1473	0.1483	--	**0.1564**	0.1492
	overload	0.1401	0.1410	--	**0.1485**	0.1418
4-5	nominal	--	0.1438	0.1491	**0.1518**	0.1461
	overload	--	0.1255	**0.1399**	0.1339	0.1308

The most important point to be noted from the results is that the best possible locations for compensator placement (in terms of improvement of transient stability) may be different in an overloaded system from those in the nominally loaded system for some of the cases. For example, for a fault in line 8-7 (with $\alpha 145°$ and $I_{\max} = 1.0$), the best locations in the overloaded system are the same as the best locations for nominally loaded system (line 5-7 for TCSC and line 6-9 for STATCOM) when the overloading is done at bus 6. However, for overloading at bus 8, the best locations for overloaded system (line 5-7 for TCSC and line 8-9 for STATCOM) are different from those of the nominally loaded system. Again, from Table XI, it can be seen that for a fault in line 8-9 and the TCSC placed in line 5-7, the best possible location of the STATCOM is line 6-9 for both nominally loaded and overloaded system. However, for a fault in the same line and TCSC in line 4-5, the best possible location of STATCOM changes from line 6-9 in nominally loaded system to line 5-7 in overloaded system.

A summary of the observations of this section is presented below.

- It is found that in some cases, the best-suited placement locations of the compensators for simultaneous use of the

devices are different from the suitable locations for their individual use.
- The effects of FACTS devices on a stressed system may vary from those in a nominally loaded system.
- Therefore, separate assessments of transient stability are to be done for combined application of two FACTS devices in different operating conditions. TS and η can help in making that assessment.

VI. Conclusion

This paper presents the trajectory sensitivity analysis of a power system compensated by series and shunt FACTS devices like TCSC and STATCOM. TSA is used here to assess the transient stability condition of the system. The inverse of the maximum value of the norm of the sensitivities of all the states (η) is used as a measure of transient stability margin. This obviates the need for doing repeated simulations up to $t_{\rm cr}$. At any operating condition, an idea about the system's distance from instability can be obtained by computing η. Thus, the number of simulations to be done reduces considerably. The value of $t_{\rm cr}$ can also be estimated using this method. One of the generators has been taken here as the reference. It has been shown that COI can also be used as reference, and the results in these two cases provide similar information.

A comparative study of variation of transient stability condition on application of TCSC and STATCOM individually vis-á-vis the effect of their simultaneous application has been made. The best possible locations of the FACTS devices are found to vary with the location of the fault and the operating criteria of the devices. TS and η can be used to identify these locations. In some cases, the FACTS device may have some adverse effect on system stability. Also an increase in compensation by the FACTS devices does not ensure an enhanced stability margin. Therefore, evaluation of the system stability condition is required for better and safer system operation. This evaluation can be done using TS. The best possible location for stability improvement for simultaneous placement of the devices may differ from the best locations for individual placement. Therefore, separate stability assessment is needed for the simultaneous operation of the compensators. Also the best possible locations of the devices change in a stressed system. All these underline the importance of a tool for transient stability assessment like trajectory sensitivity.

Acknowledgment

The authors would like to thank Prof. M.A. Pai of the University of Illinois at Urbana-Champaign for his valuable suggestions and constructive criticism on this paper.

References

[1] V. Vittal, E.-Z. Zhou, C. Hwang, and A. A. Fouad, "Derivation of stability limits using analytical sensitivity of the transient energy margin," *IEEE Trans. Power Syst.*, vol. 4, no. 4, pp. 1363–1372, Nov.. 1989.
[2] K. N. Shubhanga and A. M. Kulkarni, "Application of structure preserving energy margin sensitivity to determine the effectiveness of shunt and series FACTS devices," *IEEE Trans. Power Syst.*, vol. 17, no. 3, pp. 730–738, Aug. 2002.
[3] M. J. Laufenberg and M. A. Pai, "A new approach to dynamic security assessment using trajectory sensitivities," *IEEE Trans. Power Syst.*, vol. 13, no. 3, pp. 953–958, Aug. 1998.
[4] T. B. Nguyen, "Dynamic security assessment of power systems using trajectory sensitivity approach," Ph.D. dissertation, Dept. Elect. Comput. Eng., Univ. Illinois at Urbana-Champaign, Urbana, IL, 2002.
[5] I. A. Hiskens and M. A. Pai, "Trajectory sensitivity analysis of hybrid systems," *IEEE Trans. Circuits Syst I, Fundam. Theory Appl.*, vol. 47, no. 2, pp. 204–220, Feb. 2000.
[6] S. A. Soman, T. B. Nguyen, M. A. Pai, and R. Vaidyanathan, "Analysis of angle stability problems: a transmission protection systems perspective," *IEEE Trans. Power Del.*, vol. 19, no. 3, pp. 1024–1033, Jul. 2004.
[7] K. N. Shubhanga and A. M. Kulkarni, "Determination of effectiveness of transient stability controls using reduced number of trajectory sensitivity computations," *IEEE Trans. Power Syst.*, vol. 19, no. 1, pp. 473–482, Feb. 2004.
[8] K. R. Padiyar and A. L. Devi, "Control and simulation of static condenser," in *Proc. 9th Annu. Applied Power Electronics Conf. Expo.*, Feb. 13-17, 1994.
[9] K. R. Padiyar and K. U. Rao, "Discrete control of TCSC for stability improvement in power systems," in *Proc. 4th IEEE Conf. Control Applications*, Sep. 28-29, 1995.
[10] P. W. Sauer and M. A. Pai, *Power System Dynamics and Stability*. Upper Saddle River, NJ: Prentice-Hall, 1998.
[11] Power System Toolbox, Version 2.0, Cherry Tree Scientific Software.
[12] P. Kundur, *Power System Stability and Control*. New York: McGraw-Hill, 1994.
[13] K. R. Padiyar, *Power System Dynamics, Stability and Control*. Hyderabad, India: BS Publications, 2002.
[14] P. M. Anderson and A. A. Fouad, *Power System Stability and Control*. Ames, IA: Iowa State Univ. Press, 1977.
[15] N. Christl, R. Hedin, P. E. Krause, and S. M. McKenna, "Advanced series compensation (ASC) with thyristor controlled impedance," in *Proc. CIGRE General Session*, 1992.
[16] N. G. Hingorani and L. Gyugyi, *Understanding FACTS*. Delhi, India: Standard Publishers Distributors, 2001.
[17] C. A. Canizares, "Power flow and transient stability models of FACTS controllers for voltage and angle stability studies," in *Proc. IEEE Power Eng. Soc. Winter Meeting*, Singapore, Jan. 23-27, 2000, vol. 2, pp. 1447–1452.

Dheeman Chatterjee (S'04) received the B.E. and M.E. degrees in electrical engineering from Bengal Engineering College, Howrah, W.B., India, in 1996 and 2002, respectively. He is currently pursuing the Ph.D. degree at the Department of Electrical Engineering, IIT Kanpur, Uttar Pradesh, India.

His area of interest is power system studies.

Arindam Ghosh (S'80–M'83–SM'93–F'06) received the Ph.D. degree in electrical engineering from University of Calgary, Calgary, AB, Canada, in 1983.

Currently, he is a Professor of power engineering at Queensland University of Technology, Brisbane, Australia. Prior to this, he was with IIT Kanpur, Uttar Pradesh, India, for 21 years. His interests are in control of power systems and power electronic devices.